Field-induced spin exciton doublet splitting in $d_{x^2-y^2}$-wave CeMIn$_5$(M = Rh,Ir,Co) heavy-electron superconductors

Alireza Akbari* and Peter Thalmeier
Max Planck Institute for the Chemical Physics of Solids, Dresden D-01187, Germany
(Received 14 August 2012; published 12 October 2012)

We investigate the spin exciton modes in the superconducting $d_{x^2-y^2}$ state of CeMIn$_5$ heavy-fermion compounds found at the antiferromagnetic wave vector by inelastic neutron scattering. We present a theoretical model that explains the field dependence for both field directions. We show that the recently observed splitting of the spin exciton doublet in CeCoIn$_5$ into two nondegenerate modes for an in-plane field appears naturally in this model. This is due to the spin anisotropy of g factors and quasiparticle interactions, which lead to different resonant conditions for the dynamic susceptibility components. We predict that the splitting of the spin-resonance doublet becomes strongly nonlinear for larger fields when the energy of both split components decreases. For a field along the tetragonal axis, no splitting but only a broadening of the resonance is found in agreement with the experiment.

DOI: 10.1103/PhysRevB.86.134516 PACS number(s): 74.25.Jb, 71.27.+a, 72.15.Qm

I. INTRODUCTION

In unconventional superconductors, quasiparticle excitations that determine low-temperature thermodynamics and response exhibit a generally anisotropic gap $\Delta(\mathbf{k})$ with possible node lines on the Fermi surface (FS). In addition to these single-particle excitations, collective excitations may appear. The collective oscillation of the superfluid density or "Higgs mode" that belongs to the singlet spin sector is difficult to observe. In addition, collective spin triplet excitations may be present below the gap edges that are formed as bound states due to quasiparticle interactions. They are accessible directly by inelastic neutron scattering (INS) and have been found in a considerable number of unconventional superconductors. In heavy-fermion compounds, their typical energies are in the range of just 1 meV. The most clear-cut example belongs to the class of 115 superconductors CeMIn$_5$ (M = Rh, Ir, and Co). They have attracted great interest because of coexisting and competing antiferromagnetic (AF) and superconducting (SC) states,[1–4] and, in particular, due to the possible existence of a Fulde-Ferrell-Larkin-Ovchinnikov (FFLO) phase in CeCoIn$_5$.[5]

The highest superconducting critical temperature of this family appears in CeCoIn$_5$ with $T_c = 2.3$ K, and the question of the gap symmetry in these compounds has been intensely discussed.[6–8] A powerful indirect method to study the unconventional gap symmetry is provided by the spin-resonance peak, which may appear in INS. Such a pronounced spin resonance has been observed in CeCoIn$_5$ and La-substituted crystals at $\omega_r/2\Delta_1 = 0.65$ in the superconducting state by INS where $2\Delta_1$ is the main quasiparticle gap obtained from tunneling experiments.[9] It is confined to a narrow region around the AF wave vector $\mathbf{Q} = (\frac{1}{2}, \frac{1}{2}, \frac{1}{2})$.[10] A theoretical calculation of the dynamical spin response using a realistic Fermi surface[11] shows that the resonance can appear only for the $d_{x^2-y^2}$-wave gap symmetry but not for the d_{xy}-type gap because the precondition $\Delta(\mathbf{k}+\mathbf{Q}) = -\Delta(\mathbf{k})$ for a spin resonance[12] is only fulfilled in the former case. Indeed, the $d_{x^2-y^2}$ gap symmetry has also been found by thermal conductivity[7] and specific heat measurements[8] in rotating magnetic fields.

The existence of a spin exciton resonance in the SC phase is a well-established many-body effect, which has also been observed in other unconventional superconductors, such as high-T_c cuprates,[13] heavy-fermion metals UPd$_2$Al$_3$ (Refs. 14–16) and CeCu$_2$Si$_2$ (Refs. 17 and 18) and, in particular, in many Fe-pnictide compounds.[19] The appearance of the resonance depends sensitively on the type of unconventional Cooper pairing and provides a powerful criterion to eliminate certain forms of pairing when a resonance is observed. These interpretations, however, all depend considerably on theoretical phenomenological model features, such as FS nesting properties, nodal positions, and momentum dependence of the gap as well as the size and anisotropy of quasiparticle interactions.

The spin exciton is a triplet excitation in the isotropic case since it should appear as a pole or resonance in all three components of the susceptibility tensor. In principle, in the presence of the magnetic field, it should split into three modes with different polarizations (left and right handed as well as longitudinal). The field-induced splitting of spin excitons has been predicted for the cuprates[20] but, so far, was never identified experimentally in these unconventional superconductors.

Recently, an apparent field-induced spin exciton splitting was found for the first time in CeCoIn$_5$ by INS and gave rise to an interesting debate. In Ref. 21, a splitting into two (rather than the expected three) modes was found for the field in the tetragonal plane, and no splitting was found for the perpendicular field. On the other hand, no splitting was reported in Refs. 22 and 23 for both field directions, and only an increased broadening of the peak was observed.[22] Furthermore, it has been proposed that the FFLO-type inhomogeneous superconducting "**Q** phase"[24–27] is due to the condensation of the lower split-off branch of spin excitons close to the upper critical field.[21,28]

In this paper, we present a theoretical analysis to address the field splitting of the spin resonance, which was recently observed in INS experiments[21] for the first time in an unconventional superconductor. We investigate whether the conventional picture of this mode as a triplet bound state of

quasiparticles can explain these observations. We clarify the appropriate conditions for the splitting to occur for the different field directions as well as the number and field dependence of the split spin exciton modes.

II. THEORETICAL MODEL

The Anderson lattice model provides a convenient frame to model the heavy quasiparticle bands in CeMIn$_5$ realistically.[29] The electronic structure of CeMIn$_5$ has been investigated by using tight-binding models with effective hybridization for f electrons and c (conduction) electrons.[29,30] The crystalline electric-field (CEF) splitting is approximately three times larger than the quasiparticle band width ($W \approx 4$ meV), and then one may restrict the model to consider the lowest $\Gamma_7^{(1)}$ Kramers doublet of $4f$ states.[31] This can be described by a pseudospin $\sigma = \uparrow\downarrow$ degree of freedom. Choosing its quantization axis along the $\hat{z}$ direction, which is defined by the magnetic field, the Anderson lattice model Hamiltonian for the two hybridized conduction and localized orbitals (c, f), which are doubly Kramers degenerate is given by

$$\mathcal{H} = \sum_{\mathbf{k}\sigma} \varepsilon^c_{\mathbf{k}\sigma} c^\dagger_{\mathbf{k}\sigma} c_{\mathbf{k}\sigma} + \varepsilon^f_{\mathbf{k}\sigma} f^\dagger_{\mathbf{k}\sigma} f_{\mathbf{k}\sigma} + V_{\mathbf{k}}(c^\dagger_{\mathbf{k}\sigma} f_{\mathbf{k}\sigma} + \text{H.c.}) + \sum_{\mathbf{k}\mathbf{k}'} U_{ff} f^\dagger_{\mathbf{k}\uparrow} f_{\mathbf{k}\uparrow} f^\dagger_{\mathbf{k}'\downarrow} f_{\mathbf{k}'\downarrow}, \quad (1)$$

where $c^\dagger_{\mathbf{k}\sigma}$ creates an electron with spin σ in the conduction orbital with wave vector $\mathbf{k} = (k_x, k_y, k_z)$. Furthermore, $\varepsilon^c_{\mathbf{k}\sigma} = \epsilon^c_{\mathbf{k}} - \mathcal{H}^c_B$ and $\varepsilon^f_{\mathbf{k}\sigma} = \epsilon^f_{\mathbf{k}} - \mathcal{H}^f_B$, where $\epsilon^c_{\mathbf{k}}$ and $\epsilon^f_{\mathbf{k}}$ are effective tight-binding dispersions of the conduction band and the renormalized dispersion for the f band, respectively. The Zeeman splittings of bands due to the effective molecular fields are given by $\mathcal{H}^c_B = h^c_B \sigma_z$ with $h^c_B = \frac{1}{2} g^c \tilde{\chi} \mu_B B$ and $\mathcal{H}^f_B = h^f_B \sigma_z$ with $h^f_B = \frac{1}{2} g^f_\alpha \tilde{\chi} \mu_B B$. Here, σ_z is the Pauli matrix, B is the magnetic field, g^c is the g factor for c electrons, g^f_α is the g factor for the f electrons in direction $\alpha = \parallel, \perp$ with respect to the tetragonal plane, $\tilde{\chi}$ is the Stoner enhancement factor of the homogeneous susceptibility due to quasiparticle interactions, and μ_B is the Bohr magneton. The anisotropy of the g factors is obtained from that of magnetization or spin susceptibility[32] as $g^f_\perp / g^f_\parallel = 2.3$ assuming that the f-electron contribution in the magnetization dominates. For that reason, we chose a small $g^c / g^f_\parallel = 0.2$. Furthermore, $f^\dagger_{\mathbf{k}\sigma}$ creates the f electron with momentum $\mathbf{k}$ and pseudospin σ, and U_{ff} is its on-site Coulomb repulsion. Finally, $V_{\mathbf{k}}$ is the hybridization energy between the lowest $4f$ doublet and the conduction bands, which implicitly contains the effect of spin orbit and the CEF term and is taken as momentum independent.

It is known[29] that, in the limit of $U_{ff} \to \infty$ where double occupation of the f states is excluded, an auxiliary boson defines the mean-field (MF) Hamiltonian as

$$\mathcal{H} = \sum_{\mathbf{k}\sigma} \varepsilon^c_{\mathbf{k}\sigma} c^\dagger_{\mathbf{k}\sigma} c_{\mathbf{k}\sigma} + \tilde{\varepsilon}^f_{\mathbf{k}\sigma} f^\dagger_{\mathbf{k}\sigma} f_{\mathbf{k}\sigma} + \tilde{V}_{\mathbf{k}}(c^\dagger_{\mathbf{k}\sigma} f_{\mathbf{k}\sigma} + \text{H.c.}) + \lambda(r^2 - 1), \quad (2)$$

where $\tilde{V}_{\mathbf{k}} = V_{\mathbf{k}} r$ is the effective hybridization obtained by projecting out double occupancies ($r^2 = 1 - n_f$) and $\tilde{\varepsilon}^f_{\mathbf{k}\sigma} = \varepsilon^f_{\mathbf{k}\sigma} + \lambda$.[33,34] The MF Hamiltonian can be diagonalized using the unitary transformation,

$$f_{\mathbf{k}\sigma} = u_{+,\mathbf{k}\sigma} \alpha_{+,\mathbf{k}\sigma} + u_{-,\mathbf{k}\sigma} \alpha_{-,\mathbf{k}\sigma}, \qquad c_{\mathbf{k}\sigma} = u_{-,\mathbf{k}\sigma} \alpha_{+,\mathbf{k}\sigma} - u_{+,\mathbf{k}\sigma} \alpha_{-,\mathbf{k}\sigma}, \quad (3)$$

and, as a result, one can find the MF quasiparticle Hamiltonian as

$$\mathcal{H}^{\text{MF}} = \sum_{\pm,\mathbf{k}\sigma} E^\pm_{\mathbf{k}\sigma} \alpha^\dagger_{\pm,\mathbf{k}\sigma} \alpha_{\pm,\mathbf{k}\sigma}, + \lambda(r^2 - 1), \quad (4)$$

where the two pairs of quasiparticle bands (pairwise degenerate for the zero field) are given by

$$E^\pm_{\mathbf{k}\sigma} = \tfrac{1}{2}\left[\varepsilon^c_{\mathbf{k}\sigma} + \tilde{\varepsilon}^f_{\mathbf{k}\sigma} \pm \sqrt{\left(\varepsilon^c_{\mathbf{k}\sigma} - \tilde{\varepsilon}^f_{\mathbf{k}\sigma}\right)^2 + 4\tilde{V}^2_{\mathbf{k}}}\right], \quad (5)$$

and the quasiparticle mixing amplitudes are obtained from

$$u^2_{\pm,\mathbf{k}\sigma} = \frac{1}{2}\left(1 \pm \frac{\varepsilon^c_{\mathbf{k}\sigma} - \tilde{\varepsilon}^f_{\mathbf{k}\sigma}}{\sqrt{\left(\varepsilon^c_{\mathbf{k}\sigma} - \tilde{\varepsilon}^f_{\mathbf{k}\sigma}\right)^2 + 4\tilde{V}^2_{\mathbf{k}}}}\right). \quad (6)$$

Using the parameters defined in Ref. 29 for the above quasiparticle band structure, we plot the corresponding FS in Fig. 1(a) in the absence of a magnetic field. Since the Fermi level is located in the lower band $E^-_{\mathbf{k}\sigma}$, we can neglect the upper band $E^+_{\mathbf{k}\sigma}$ for discussing the low-energy spin excitations.

The superconducting pairs are then formed from the heavy quasiparticles of the lower band leading to a pairing potential in the Hamiltonian according to

$$\mathcal{H}^{\text{SC}} = \sum_{\mathbf{k}} \Delta_{\mathbf{k}} (\alpha^\dagger_{-,\mathbf{k}\uparrow} \alpha^\dagger_{-,-\mathbf{k}\downarrow} + \text{H.c.}), \quad (7)$$

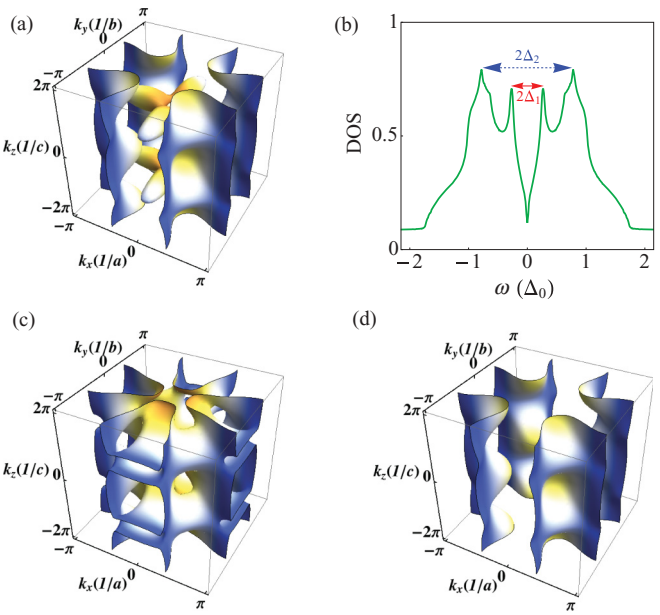

FIG. 1. (Color online) (a) Fermi surface and (b) quasiparticle density of states for a zero magnetic field, here, $2\Delta_1 = 0.56\Delta_0$ and $2\Delta_2 = 1.5\Delta_0$. (c) and (d) show Fermi surfaces for spin up and spin down, respectively, in the presence of the magnetic field $B_0\hat{z}$, corresponding to Zeeman energy splitting $h^f_{B_0} = g^f_\parallel \tilde{\chi} \mu_B B_0 = 0.3\Delta_0$, which is also used in subsequent figures.

where $\Delta_{\mathbf{k}}$ is the superconducting d-wave gap function for CeMIn$_5$ given by

$$\Delta_{\mathbf{k}} = \frac{\Delta_0}{2}(\cos k_x - \cos k_y). \tag{8}$$

By defining the new Nambu spinors as $\hat{\psi}^{\dagger}_{\mathbf{k}} = (\hat{\phi}^{\dagger}_{1\mathbf{k}}, \hat{\phi}^{\dagger}_{2\mathbf{k}})$, the effective Hamiltonian can be written as

$$\mathcal{H}^{\text{eff}} = \frac{1}{2}\sum_{\mathbf{k}} \hat{\psi}^{\dagger}_{\mathbf{k}} \hat{\beta}_{\mathbf{k}} \hat{\psi}_{\mathbf{k}}. \tag{9}$$

Here, $\hat{\phi}^{\dagger}_{1\mathbf{k}} = (\alpha^{\dagger}_{-,\mathbf{k}\uparrow}, \alpha^{\dagger}_{-,\mathbf{k}\downarrow})$,
$\hat{\phi}^{\dagger}_{2\mathbf{k}} = (\alpha_{-,-\mathbf{k}\uparrow}, \alpha_{-,-\mathbf{k}\downarrow})$, and

$$\hat{\beta}_{\mathbf{k}} = \begin{bmatrix} E^{-}_{\mathbf{k}\uparrow} & 0 & 0 & \Delta_{\mathbf{k}} \\ 0 & E^{-}_{\mathbf{k}\downarrow} & -\Delta_{\mathbf{k}} & 0 \\ 0 & -\Delta_{\mathbf{k}} & -E^{-}_{-\mathbf{k}\uparrow} & 0 \\ \Delta_{\mathbf{k}} & 0 & 0 & -E^{-}_{-\mathbf{k}\downarrow} \end{bmatrix}. \tag{10}$$

The propagator matrix of the conduction electrons in terms of the Nambu spinor in the Matsubara representation is obtained as $\hat{G}(\mathbf{k},\tau) = -\langle T\hat{\psi}_{\mathbf{k}}(\tau)\hat{\psi}^{\dagger}_{\mathbf{k}}(0)\rangle$. Using a standard equation-of-motion method, one can find that

$$\hat{G}(\mathbf{k},\omega_n) = (i\omega_n - \hat{\beta}_{\mathbf{k}})^{-1}. \tag{11}$$

Explicitly written,

$$\hat{G}(\mathbf{k},\tau) = \begin{bmatrix} \hat{G}^{11}_0(\mathbf{k},\tau) & \hat{G}^{12}_0(\mathbf{k},\tau) \\ \hat{G}^{21}_0(\mathbf{k},\tau) & \hat{G}^{22}_0(\mathbf{k},\tau) \end{bmatrix}, \tag{12}$$

where $\hat{G}^{\varsigma\varsigma'}_0(\mathbf{k},\tau) = -\langle T\hat{\phi}_{\varsigma\mathbf{k}}(\tau)\hat{\phi}^{\dagger}_{\varsigma'\mathbf{k}}(0)\rangle$ and $\varsigma,\varsigma' = 1,2$ denote the spinor components for $\pm\mathbf{k}$ below Eq. (9).

A. Magnetic susceptibility

The noninteracting or bare dynamical f-electron susceptibility is defined by

$$\chi^{ll'}_{\mathbf{q}}(\tau) = -\theta(\tau)\langle T j^{l}_{\mathbf{q}}(\tau) j^{l'}_{-\mathbf{q}}(0)\rangle, \tag{13}$$

where

$$j^{l}_{\mathbf{q}} = \sum_{\mathbf{k}\sigma\sigma'} f^{\dagger}_{\mathbf{k}+\mathbf{q}\sigma} \hat{M}^{l}_{\sigma\sigma'} f_{\mathbf{k}\sigma'}. \tag{14}$$

The hybridizing $4f$ states are in a $|\Gamma^{(1)}_7\rangle$ Kramers doublet state, and therefore, their physical moment operator (in units of μ_B) can be presented by a pseudospin matrix $\boldsymbol{\sigma}$ according to ($l = +, -, z$)

$$\hat{M}_l = m_l \sigma_l. \tag{15}$$

Here, m_l are matrix elements, and their anisotropy ($m_{\pm} = m_{\parallel}; m_z = m_{\perp}$) may be directly obtained from that of the experimental spin susceptibility of quasiparticles[32] according to $m_{\perp}/m_{\parallel} = g^{f}_{\perp}/g^{f}_{\parallel} = (\chi^{s}_{\perp}/\chi^{s}_{\parallel})^{1/2} = 2.3$. Their absolute value is not significant as it only sets the overall scale. Then, the bare physical moment susceptibility can be expressed as

$$\chi^{ll'}(\mathbf{q},\omega) = m_l m_{l'} \chi^{ll'}_0(\mathbf{q},\omega), \tag{16}$$

where $\chi^{ll'}_0(\mathbf{q},\omega)$ is the pseudospin susceptibility defined by

$$\begin{aligned}\chi^{ll'}_0(\mathbf{q},\omega) = \sum_{\mathbf{k},\{\sigma\}} &\boldsymbol{\sigma}^{l}_{\sigma\sigma'} \boldsymbol{\sigma}^{l'}_{\sigma_1\sigma_1'} u_{-,\mathbf{k}+\mathbf{q}\sigma} u_{-,\mathbf{k}+\mathbf{q}\sigma_1'} u_{-,\mathbf{k}\sigma_1} u_{-,\mathbf{k}\sigma'} \\ &\times \int d\omega' \hat{G}^{11}_{0\sigma\sigma_1'}(\mathbf{k}+\mathbf{q},\nu+\omega') \hat{G}^{11}_{0\sigma_1\sigma'}(\mathbf{k},\omega') \\ &\times |_{i\nu\to\omega+i0^+}. \end{aligned} \tag{17}$$

With the definition of the new basis as $\hat{\varphi}^{\dagger}_{\mathbf{k}} = (b_{+,1\mathbf{k}}, b_{+,2\mathbf{k}}, b_{-,2\mathbf{k}}, b_{-,1\mathbf{k}})$ and applying the Bogoliubov transformation given by

$$\begin{aligned} \alpha^{\dagger}_{-,\mathbf{k}\uparrow} &= v_{+,1\mathbf{k}} b_{+,1\mathbf{k}} + v_{-,1\mathbf{k}} b_{-,1\mathbf{k}}, \\ \alpha_{-,-\mathbf{k}\downarrow} &= -v_{-,1\mathbf{k}} b_{+,1\mathbf{k}} + v_{+,1\mathbf{k}} b_{-,1\mathbf{k}}, \\ \alpha^{\dagger}_{-,\mathbf{k}\downarrow} &= v_{+,2\mathbf{k}} b_{+,2\mathbf{k}} - v_{-,2\mathbf{k}} b_{-,2\mathbf{k}}, \\ \alpha_{-,-\mathbf{k}\uparrow} &= v_{-,2\mathbf{k}} b_{+,2\mathbf{k}} + v_{+,2\mathbf{k}} b_{-,2\mathbf{k}}, \end{aligned} \tag{18}$$

the effective Hamiltonian in Eq. (9) is diagonalized by $\hat{\beta}^{d}_{\mathbf{k}} = P_{\mathbf{k}} \hat{\beta}_{\mathbf{k}} P^{-1}_{\mathbf{k}}$, where $P_{\mathbf{k}}$ is a 4×4 matrix, composed of the eigenvectors of $\hat{\beta}_{\mathbf{k}}$. Here, $\hat{\beta}^{d}_{\mathbf{k}}$ is the diagonal matrix constructed from the corresponding eigenvalues,

$$\bar{E}^{\pm}_{1\mathbf{k}} = \bar{E}^{\pm}_{2,-\mathbf{k}} = \tfrac{1}{2}\big[E^{-}_{\mathbf{k}\uparrow} - E^{-}_{-\mathbf{k}\downarrow} \pm \sqrt{(E^{-}_{\mathbf{k}\uparrow} + E^{-}_{-\mathbf{k}\downarrow})^2 + 4\Delta^2_{\mathbf{k}}}\big], \tag{19}$$

and $P^{-1}_{\mathbf{k}}$ is the matrix inverse of $P_{\mathbf{k}}$. Furthermore,

$$v^2_{\pm,1\mathbf{k}} = v^2_{\pm,2,-\mathbf{k}} = \frac{1}{2}\left(1 \pm \frac{E^{-}_{\mathbf{k}\uparrow} + E^{-}_{-\mathbf{k}\downarrow}}{\sqrt{(E^{-}_{\mathbf{k}\uparrow} + E^{-}_{-\mathbf{k}\downarrow})^2 + 4\Delta^2_{\mathbf{k}}}}\right). \tag{20}$$

Then, $\hat{G}^{d}(\mathbf{k},\omega_n) = (i\omega_n - \hat{\beta}^{d}_{\mathbf{k}})^{-1}$ is diagonal, and we can write

$$\hat{G}^{11}_{0\sigma\sigma_1}(\mathbf{k},\omega_n) = \sum_{s'=1}^{4} \gamma^{\mathbf{k}}_{\sigma\sigma_1 s'} \hat{G}^{d}_{s'}(\mathbf{k},\omega_n), \tag{21}$$

where $\gamma^{\mathbf{k}}_{\sigma\sigma_1 s'} = P^{-1}_{\mathbf{k}\sigma s'} P_{\mathbf{k}s'\sigma_1}$. Thus, the pseudospin susceptibility can now be expressed as

$$\begin{aligned}\chi^{ll'}_0(\mathbf{q},\omega) = \sum_{\mathbf{k},\{\sigma\}} \sum_{\{s\}} &\boldsymbol{\sigma}^{l}_{\sigma\sigma'} \boldsymbol{\sigma}^{l'}_{\sigma_1\sigma_1'} \gamma^{\mathbf{k}+\mathbf{q}}_{\sigma\sigma_1' s_2} \gamma^{\mathbf{k}}_{\sigma_1\sigma' s_2'} \\ &\times u_{-,\mathbf{k}+\mathbf{q}\sigma} u_{-,\mathbf{k}+\mathbf{q}\sigma_1'} u_{-,\mathbf{k}\sigma_1} u_{-,\mathbf{k}\sigma'} \\ &\times \frac{f(\hat{\beta}^{d}_{\mathbf{k}+\mathbf{q},s_2}) - f(\hat{\beta}^{d}_{\mathbf{k},s_2'})}{\omega - (\hat{\beta}^{d}_{\mathbf{k}+\mathbf{q},s_2} - \hat{\beta}^{d}_{\mathbf{k},s_2'})}, \end{aligned} \tag{22}$$

where $f(\ldots)$ is the Fermi function. The combination of prefactors in the sum of Eq. (22) is the combined coherence factors arising from the hybridization and the superconducting state. Finally, the Cartesian dynamic magnetic susceptibility tensor in random-phase approximation (RPA) has the form

$$\hat{\chi}_{\text{RPA}}(\mathbf{q},\omega) = [1 - \hat{J}(\mathbf{q})\hat{\chi}(\mathbf{q},\omega)]^{-1}\hat{\chi}(\mathbf{q},\omega), \tag{23}$$

where $\hat{J}(\mathbf{q})$ is the effective quasiparticle interaction matrix with nonzero elements: $J^{zz}_{\mathbf{q}} = J^{\perp}_{\mathbf{q}}, J^{\pm}_{\mathbf{q}} = J^{\mp}_{\mathbf{q}} = J^{\parallel}_{\mathbf{q}}$. Similar to the g factors, they may be anisotropic. Furthermore, their momentum dependence can be modeled by a Lorentzian function, which is peaked at the wave vector $\mathbf{Q}$ associated with the indirect hybridization gap.[35] Finally, the total dynamic

magnetic susceptibility is obtained as the trace of the tensor according to

$$\chi_{\rm RPA}(\mathbf{q},\omega) = \chi^{zz}_{\rm RPA}(\mathbf{q},\omega) + \tfrac{1}{2}[\chi^{\pm}_{\rm RPA}(\mathbf{q},\omega) + \chi^{\mp}_{\rm RPA}(\mathbf{q},\omega)]. \quad (24)$$

For momentum transfer $\mathbf{q}$ along the $\mathbf{Q} = (\frac{1}{2},\frac{1}{2},\frac{1}{2})$ direction, this is directly proportional to the dynamical f-electron structure factor $S(\mathbf{q},\omega)$ observed in INS experiments. The total magnetic scattering cross section is dominated by the magnetic response of more localized f electrons because their atomic form factors are larger than those of conduction electrons for momentum transfer on the order of a reciprocal lattice vector. Therefore, only the f-electron dynamical response is considered here.

III. NUMERICAL RESULTS

In this section, we numerically evaluate the dynamic magnetic susceptibility for our model of 115 systems. We consider two different cases, namely, the magnetic field along the $\hat{z}$ direction (out of plane: c axis) and along the $\hat{x}$ direction (in plane: a axis). For clarity, we first give the relevant physical parameters of $CeCoIn_5$ to simplify comparison with experimental results.

We present the superconducting quasiparticle density of states (DOS) in Fig. 1(b). As a result of the inner and outer parts of the Fermi sheets [see Fig. 1(a)], it showed two kind of gaps, namely, the lower Δ_1 and the larger Δ_2, which were both identified in tunneling experiments.[9]

For the main (lower) tunneling gap, we have $2\Delta_1 = 0.56\Delta_0 = 0.92$ meV or $\Delta_0 = 1.64$ meV for the gap amplitude in Eq. (8). The spin-resonance energy for the zero field is $\omega_r = 0.6$ meV (Ref. 10) or $\omega_r/2\Delta_1 \simeq 0.65$.

First, using Eq. (22), we calculate the individual components $\chi_0^{ll'}(\mathbf{Q},\omega)$ of the pseudospin susceptibility tensor and its trace $\chi_0^{\rm tot}(\mathbf{Q},\omega) = \chi_0^{zz}(\mathbf{Q},\omega) + \frac{1}{2}[\chi_0^{\pm}(\mathbf{Q},\omega) + \chi_0^{\mp}(\mathbf{Q},\omega)]$. For $B \to 0$, Fig. 2(a) shows that $\frac{1}{2}\chi_0^{\pm}, \frac{1}{2}\chi_0^{\mp}$, and χ_0^{zz} become identical, independent of the field direction due to isotropy in the pseudospin space. Therefore, $\chi_0^{\rm tot}$ for $B \to 0$ in Fig. 2(a) is simply three times each of these components. This means that the anisotropy enters only through the matrix elements in the physical moment susceptibility of Eq. (16) discussed below. The pseudospin susceptibility in the presence of a magnetic field along the $\hat{z}$ direction is shown in Fig. 2(b) and for the $\hat{x}$ direction in Fig. 2(c). We note, here, that, for calculating the pseudospin susceptibility with a magnetic field along the $\hat{x}$ direction, we have applied a $\pi/2$ rotation along the $\hat{y}$ direction ($\hat{x} \to -\hat{z}$ and $\hat{z} \to \hat{x}$) and a similar one in the $\mathbf{k}$ space. For the finite field and both directions, the individual components for each field direction start to differ because of the polarization of quasiparticle bands in the field. This leads to a change in the nesting conditions of the FS in the presence of a magnetic field, shown in Figs. 1(c) and 1(d), which is different for each susceptibility component. Most importantly, the energy dependence of $\chi_0^{\pm}$ and $\chi_0^{\mp}$ shows a splitting in an opposite manner increasing with field. This is due to the chirality introduced in the response due to the splitting of quasiparticle band energies in Eq. (22).

We also calculate the total bare physical susceptibility $\chi^{\rm tot}(\mathbf{Q},\omega)$, resulting from Eq. (16), in Fig. 3. The anisotropy

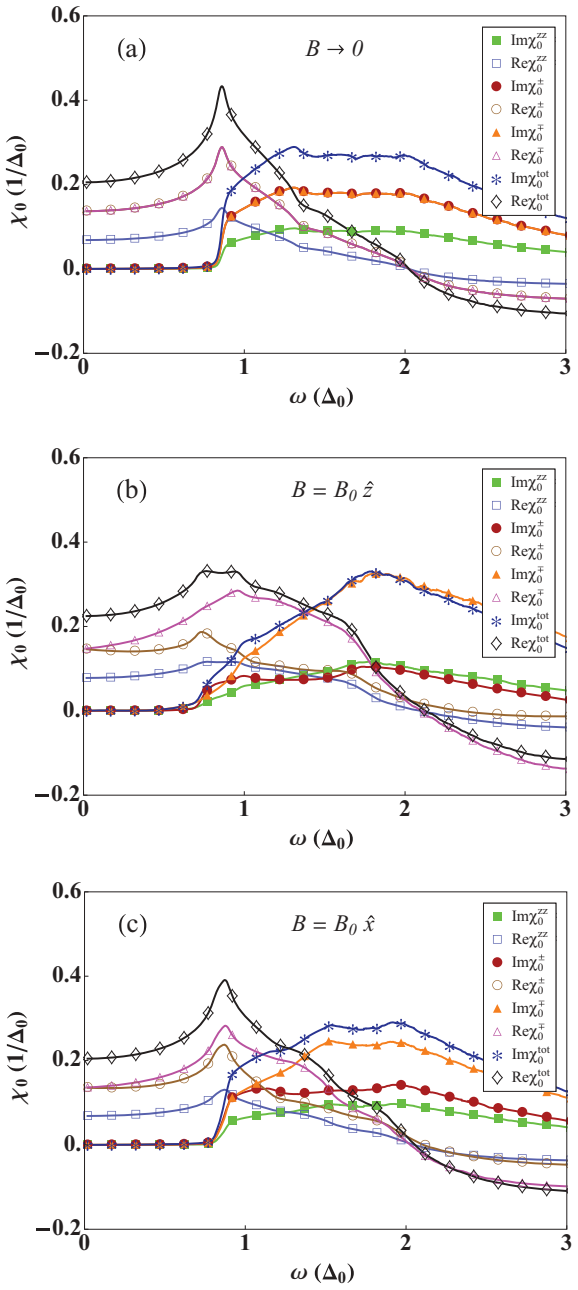

FIG. 2. (Color online) Individual components $[\chi_0^{ll'}(\mathbf{Q},\omega)]$ and total $[\chi_0^{\rm tot}(\mathbf{Q},\omega)]$ of the unperturbed pseudospin susceptibility in (a) the absence, (b) the presence of the magnetic field along the $\hat{z}$ direction, and for (c) the magnetic field along the $\hat{x}$ direction. (B_0 is the same as Fig. 1.)

enters only through the matrix elements $m_{\parallel}, m_{\perp}$ in the physical moment susceptibility of Eq. (16). It is shown at zero magnetic field ($B \to 0$) and for the magnetic field along the $\hat{z}$ and $\hat{x}$ directions (in the original axis notation), respectively. We note that, for $B \to 0$, the $\frac{1}{2}\chi^{\pm}$ and $\frac{1}{2}\chi^{\mp}$ components are still equivalent as in Fig. 2(a) but differ from χ^{zz} due to the different magnetic moments for in-plane and out-of-plane directions [see Eq. (15)].

Finally, from Eq. (25), the interacting RPA susceptibility and the spectrum of excitations given by its imaginary part

can be calculated. In general form, we obtain

$$\chi_{\mathrm{RPA}}(\mathbf{q},\omega)=\frac{m_z^2\chi_0^{zz}}{1-\lambda_z\chi_0^{zz}}+\frac{(m_x^2+m_y^2)(\chi_0^{\pm}+\chi_0^{\mp})-(\lambda_x m_y^2+\lambda_y m_x^2)\chi_0^{\pm}\chi_0^{\mp}}{4-(\lambda_x+\lambda_y)(\chi_0^{\pm}+\chi_0^{\mp})+\lambda_x\lambda_y\chi_0^{\pm}\chi_0^{\mp}}, \tag{25}$$

where the interaction parameters are defined as $\lambda_l=m_l^2J_{\mathbf{q}}^l$. Explicitly, for field $\mathbf{B}$ in the ab plane with rotated axes ($l=z=y=\|\,,x=\perp$), we have

$$\chi_{\mathrm{RPA}}(\mathbf{q},\omega)=\frac{m_\|^2\chi_0^{zz}}{1-\lambda_\|\chi_0^{zz}}+\frac{(m_\|^2+m_\perp^2)(\chi_0^{\pm}+\chi_0^{\mp})-(\lambda_\| m_\perp^2+\lambda_\perp m_\|^2)\chi_0^{\pm}\chi_0^{\mp}}{4-(\lambda_\|+\lambda_\perp)(\chi_0^{\pm}+\chi_0^{\mp})+\lambda_\perp\lambda_\|\chi_0^{\pm}\chi_0^{\mp}}, \tag{26}$$

and, for field $\mathbf{B}$ along the c direction with original axes ($l=x=y=\|\,,z=\perp$), one obtains

$$\chi_{\mathrm{RPA}}(\mathbf{q},\omega)=\frac{m_\perp^2\chi_0^{zz}}{1-\lambda_\perp\chi_0^{zz}}+\frac{m_\|^2\chi_0^{\pm}}{2-\lambda_\|\chi_0^{\pm}}+\frac{m_\|^2\chi_0^{\mp}}{2-\lambda_\|\chi_0^{\mp}}. \tag{27}$$

If the resonance condition should be satisfied for both transverse parts in Eq. (26), then one must have $m_\|^2J_{\mathbf{q}}^{\perp}\approx m_\perp^2J_{\mathbf{q}}^{\|}$. Since the CEF states and, hence, the anisotropy may change as an effect of substitutions in the pure 115 compounds, the resonance signatures may also change accordingly. As a result of the sign change in the superconducting gap function ($\Delta_{\mathbf{k}+\mathbf{Q}}=-\Delta_{\mathbf{k}}$) at the antiferromagnetic momentum $\mathbf{Q}$, the spectral function $\mathrm{Im}\,\chi_0(\mathbf{Q},\omega)$ remains zero for the low frequencies and then shows a discontinuous jump at the onset frequency of the particle-hole continuum, i.e., close to $\omega_c=\min(\Delta_{\mathbf{k}+\mathbf{Q}}+\Delta_{\mathbf{k}})$. This is around $\Delta_0\simeq 2\Delta_1$, where $2\Delta_1$ is the gap in the superconducting DOS in [Fig. 1(b)], which is observed in the tunneling spectrum of $CeCoIn_5$.[9] The resonance may appear for energies $\omega<\omega_c$, under the conditions that: (i) $J_{\mathbf{q}}^{ll'}\,\mathrm{Re}\,\chi_{0\mathbf{q}}^{ll'}(\omega)=1$ and (ii) $\mathrm{Im}\,\chi_{0\mathbf{q}}^{ll'}(\omega)\simeq 0$ ($ll'=\pm,\mp,zz$).

We begin our discussion of numerical results by considering the strongly anisotropic case with $J_{\mathbf{Q}}^{\perp}\ll J_{\mathbf{Q}}^{\|}$. Only in this case is the resonance condition satisfied for both $\chi_{0\mathbf{Q}}^{\pm}$ and $\chi_{0\mathbf{Q}}^{\mp}$ components and not for $\chi_{0\mathbf{Q}}^{zz}$, i.e., a resonance doublet is possible as observed in the experiment. At zero magnetic field, a single sharp peak for the degenerate resonance is observed, which is shown in Fig. 4. By applying the magnetic field, the bare $\chi_0^{\pm},\chi_0^{\mp}$ susceptibilities start to split into an upper and lower branch [Figs. 2(b) and 2(c)], and as a result, the two resonance peaks of the doublet are revealed in the RPA frequency spectrum. Because of the anisotropic interaction, these peaks are completely distinguishable for the in-plane magnetic field showing a linear Zeeman splitting for

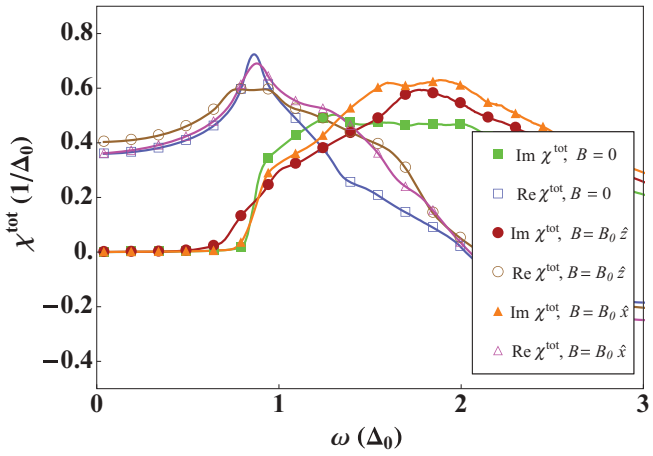

FIG. 3. (Color online) The total unperturbed physical susceptibility (including matrix elements $m_\|,m_\perp$; $\chi^{\mathrm{tot}}(\mathbf{Q},\omega)=\chi^{zz}+\frac{1}{2}[\chi^{\pm}+\chi^{\mp}]$) for the zero field and finite field along the $\hat{z}$ and $\hat{x}$ directions. (B_0 is the same as in Fig. 1.)

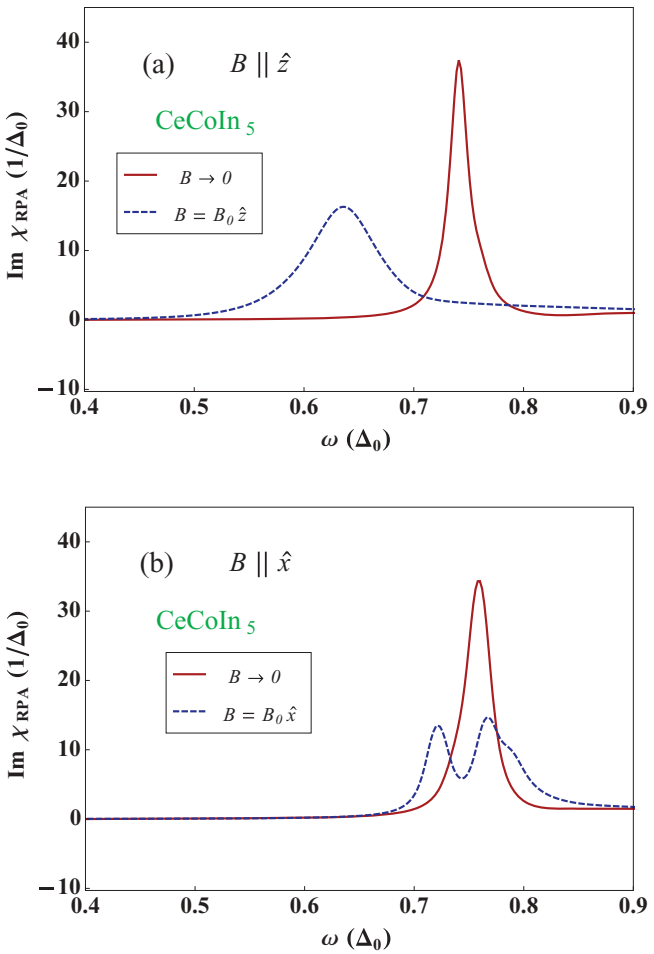

FIG. 4. (Color online) RPA susceptibility in the absence and presence of the magnetic field: (a) along the $\hat{z}$ direction and (b) along the $\hat{x}$ direction. Parameters corresponding to the behavior as observed in $CeCoIn_5$ with $g_f^{\perp}/g_f^{\|}=2.3$ and $J_{\mathbf{Q}}^{\perp}=2.6\Delta_0$; $J_{\mathbf{Q}}^{\|}=13.5\Delta_0$. ($B_0$ is the same as in Fig. 1.)

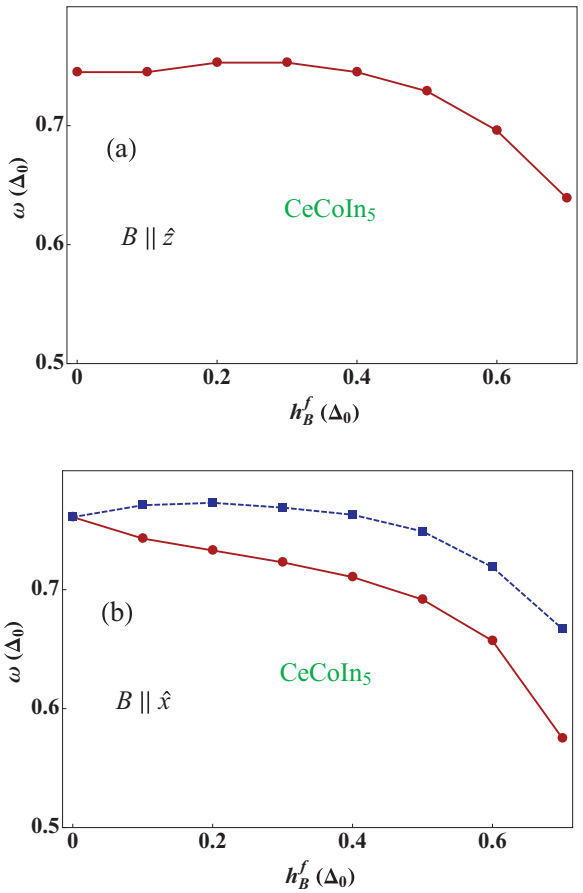

FIG. 5. (Color online) RPA susceptibility peak positions corresponding to spin-resonance energies as function of field strength: (a) along the $\hat{z}$ direction and (b) along the $\hat{x}$ direction. Anisotropic g factors with $g_f^{\perp}/g_f^{\parallel} = 2.3$ and quasiparticle interaction parameters $J_{\mathbf{Q}}^{\perp} = 2.6\Delta_0$; $J_{\mathbf{Q}}^{\parallel} = 13.5\Delta_0$, leading to similar behavior as in $CeCoIn_5$ for both field directions. Here, the maximum $h_B^f = 0.7\Delta_0$ corresponds to a field $B = 39.7/(g_f^l\tilde{\chi})$ in Teslas for direction $l = \perp, \parallel$.

small fields. On the other hand, they merge together for the out-of-plane field, and a single broadened peak appears whose width increases with the field. Using the procedure described above for various fields, we obtain the peak positions of the RPA spectrum versus magnetic-field strength in Fig. 5. For the field oriented along the $\hat{z}$ direction [Fig. 5(a)], we always have a single peak with a larger broadening, and by increasing the magnetic field, the peak moves to lower energies. But for the magnetic field applied in the $\hat{x}$ direction [Fig. 5(b)], the RPA result always shows two peaks with narrower linewidths. When the field is increased, these peaks first show a linear Zeeman splitting, and one of them moves to larger energies and the other one to lower energies. Finally, at large fields, nonlinear behavior sets in, and both start to move to lower energies. These results are in complete qualitative agreement with the experimental observation for $CeCoIn_5$ (Ref. 21) at lower fields, which so far, only have been used. It is clear that the linear splitting observed must be modified when larger fields closer to the upper critical fields are applied. The absolute field scale at the maximum $h_B^f = 0.7\Delta_0$ is $B = 39.7/(g_f^l\tilde{\chi})$ in Teslas for direction $l = \parallel, \perp$. From a comparison with the experimental linear splitting region up to 6T $\ll H_{c2}^{\parallel}$ and the one in Fig. 5(a) with $h_B^f \approx 0.35$, one gets the parameter $g_f^{\parallel}\tilde{\chi} = 3.3$. We note that the reference scale Δ_0 is only constant for fields smaller than the upper critical field ($H_{c2}^{\parallel} = 11.9, H_{c2}^{\perp} = 4.95$ T). For larger fields, one has to scale with $\Delta_0(B)$, which vanishes at the upper critical fields $H_{c2}^{\parallel,\perp}$ where the resonance energies $\omega_r(B)$ also have to vanish for both field directions. When the curves in Figs. 5(a) and 5(b) are multiplied by the scaling function $\Delta_0(B)$, the field dependence $\omega_r(B)$ is obtained in absolute (meV) units.

Finally, we mention here that our results within the phenomenological RPA theory depend on the model parameters, i.e., anisotropic matrix elements and quasiparticle interaction energies. Changing these parameters leads to other interesting regimes where the anisotropies of the magnetic moment and quasiparticle interaction along the tetragonal axes play the decisive role. The RPA treatment shows that, even in the absence of the magnetic field, an additional peak from the $\chi_{0\mathbf{q}}^{zz}$ component may appear for suitable parameters, and therefore, in principle, two peaks may exist in the RPA spectrum even at a zero field. In the presence of the magnetic field, such as the previous cases, the degenerate (doublet) peak of the $\chi_{0\mathbf{q}}^{\pm}$ and $\chi_{0\mathbf{q}}^{\mp}$ components splits and, finally, leads to three different peaks at the finite field. We should stress here that, by moving to a lower interaction energy, the resonance occurs just for $\chi_{0\mathbf{q}}^{\mp}$, and the splitting of the resonance vanishes. This could give an insight into the challenging alternative experiments where the splitting behavior for the in-plane field has not been seen.[22]

IV. CONCLUSION

We have given an explanation of the observed field splitting of feedback spin-resonance excitations recently observed for the first time in the unconventional superconductor $CeCoIn_5$. Our calculations are based on a RPA model with tetragonal anisotropy for collective spin excitations that may also be relevant for other members of the 115 family. Using the appropriate hybridized bands and associated Fermi surface as well as the proper $d_{x^2-y^2}$ superconducting gap symmetry, the spin resonance appears at $\omega/2\Delta_1 = 0.73$, close to the experimental value. Here, $2\Delta_1$ is the main tunneling gap indicated in the DOS of Fig. 1(b) and is found in Ref. 9.

In the isotropic case, the resonance is a spin triplet excitation that should split into three modes in a field as predicted in the case of a cuprate model.[20] However, because of the presence of strong CEF and hybridization-induced anisotropies of g factors and interactions of $4f$-type quasiparticles in the 115 compounds, the resonance condition may, in this case, not be fulfilled for all three triplet components. For sufficiently strong anisotropy, the zero-field resonance is only a twofold degenerate transverse doublet state because the longitudinal component does not satisfy the resonance condition. For the field in the tetragonal plane, the doublet splits with a linear Zeeman effect for low fields, one branch moving to higher, and the other branch moving to lower energies. However, for larger fields, a crossover to nonlinear field dependence with both split resonance energies decreasing sets in. For the field perpendicular to the tetragonal plane, no splitting but only a broadening of the doublet resonance excitation appears. These

salient features of our model calculation correspond closely to the experimental observations in $CeCoIn_5$ performed for small fields.[21] It would be very interesting to investigate the predicted nonlinear field dependence for larger fields.

Finally, we note that other scenarios are possible depending on the anisotropies and strengths of quasiparticle interactions where, for example, the in-plane splitting of the resonance disappears and a single peak with anomalous broadening as for the out-of-plane field is observed. In fact, this behavior was proposed in an alternative experiment,[22] and further experimental as well as theoretical investigations are necessary to clarify this issue.

*akbari@cpfs.mpg.de

[1] J. Thompson, R. Movshovich, Z. Fisk, F. Bouquet, N. Curro, R. Fisher, P. Hammel, H. Hegger, M. Hundley, M. Jaime, P. Pagliuso, C. Petrovic, N. Phillips, and J. Sarrao, J. Magn. Magn. Mater. **226-230**, 5 (2001).

[2] V. S. Zapf, E. J. Freeman, E. D. Bauer, J. Petricka, C. Sirvent, N. A. Frederick, R. P. Dickey, and M. B. Maple, Phys. Rev. B **65**, 014506 (2001).

[3] J. L. Sarrao and J. D. Thompson, J. Phys. Soc. Jpn. **76**, 051013 (2007).

[4] J. D. Thompson and Z. Fisk, J. Phys. Soc. Jpn. **81**, 011002 (2012).

[5] A. Bianchi, R. Movshovich, C. Capan, P. G. Pagliuso, and J. L. Sarrao, Phys. Rev. Lett. **91**, 187004 (2003).

[6] C. Petrovic, P. G. Pagliuso, M. F. Hundley, R. Movshovich, J. L. Sarrao, J. D. Thompson, Z. Fisk, and P. Monthoux, J. Phys.: Condens. Matter **13**, L337 (2001).

[7] K. Izawa, H. Yamaguchi, Y. Matsuda, H. Shishido, R. Settai, and Y. Onuki, Phys. Rev. Lett. **87**, 057002 (2001).

[8] K. An, T. Sakakibara, R. Settai, Y. Onuki, M. Hiragi, M. Ichioka, and K. Machida, Phys. Rev. Lett. **104**, 037002 (2010).

[9] P. M. C. Rourke, M. A. Tanatar, C. S. Turel, J. Berdeklis, C. Petrovic, and J. Y. T. Wei, Phys. Rev. Lett. **94**, 107005 (2005).

[10] C. Stock, C. Broholm, J. Hudis, H. J. Kang, and C. Petrovic, Phys. Rev. Lett. **100**, 087001 (2008).

[11] I. Eremin, G. Zwicknagl, P. Thalmeier, and P. Fulde, Phys. Rev. Lett. **101**, 187001 (2008).

[12] N. Bulut and D. J. Scalapino, Phys. Rev. B **53**, 5149 (1996).

[13] J. Rossat-Mignod, L. Regnault, C. Vettier, P. Bourges, P. Burlet, J. Bossy, J. Henry, and G. Lapertot, Physica C **185-189**, 86 (1991).

[14] N. K. Sato, N. Aso, K. Miyake, R. Shiina, P. Thalmeier, G. Varelogiannis, C. Geibel, F. Steglich, P. Fulde, and T. Komatsubara, Nature (London) **410**, 340 (2001).

[15] N. Metoki, Y. Haga, Y. Koike, N. Aso, and Y. Onuki, J. Phys. Soc. Jpn. **66**, 2560 (1997).

[16] J. Chang, I. Eremin, P. Thalmeier, and P. Fulde, Phys. Rev. B **75**, 024503 (2007).

[17] O. Stockert, J. Arndt, A. Schneidewind, H. Schneider, H. Jeevan, C. Geibel, F. Steglich, and M. Loewenhaupt, Physica B **403**, 973 (2008).

[18] O. Stockert, J. Arndt, E. Faulhaber, C. Geibel, H. S. Jeevan, S. Kirchner, M. Loewenhaupt, K. Schmalzl, W. Schmidt, Q. Si, and F. Steglich, Nat. Phys. **7**, 119 (2011).

[19] A. D. Christianson, E. A. Goremychkin, R. Osborn, S. Rosenkranz, M. D. Lumsden, C. D. Malliakas, I. S. Todorov, H. Claus, D. Y. Chung, M. G. Kanatzidis, R. I. Bewley, and T. Guidi, Nature (London) **456**, 930 (2008).

[20] J.-P. Ismer, I. Eremin, E. Rossi, and D. K. Morr, Phys. Rev. Lett. **99**, 047005 (2007).

[21] C. Stock, C. Broholm, Y. Zhao, F. Demmel, H. J. Kang, K. C. Rule, and C. Petrovic, Phys. Rev. Lett (in press).

[22] J. Panarin, S. Raymond, G. Lapertot, J. Flouquet, and J.-M. Mignot, Phys. Rev. B **84**, 052505 (2011).

[23] J. Panarin, S. Raymond, G. Lapertot, and J. Flouquet, J. Phys. Soc. Jpn. **78**, 113706 (2009).

[24] Y. Yanase and M. Sigrist, J. Phys. Soc. Jpn. **78**, 114715 (2009).

[25] A. Aperis, G. Varelogiannis, and P. B. Littlewood, Phys. Rev. Lett. **104**, 216403 (2010).

[26] M. Kenzelmann, S. Gerber, N. Egetenmeyer, J. L. Gavilano, T. Strässle, A. D. Bianchi, E. Ressouche, R. Movshovich, E. D. Bauer, J. L. Sarrao, and J. D. Thompson, Phys. Rev. Lett. **104**, 127001 (2010).

[27] K. Kumagai, H. Shishido, T. Shibauchi, and Y. Matsuda, Phys. Rev. Lett. **106**, 137004 (2011).

[28] V. P. Michal and V. P. Mineev, Phys. Rev. B **84**, 052508 (2011).

[29] K. Tanaka, H. Ikeda, Y. Nisikawa, and K. Yamada, J. Phys. Soc. Jpn. **75**, 024713 (2006).

[30] T. Maehira, T. Hotta, K. Ueda, and A. Hasegawa, J. Phys. Soc. Jpn. **72**, 854 (2003).

[31] A. D. Christianson, E. D. Bauer, J. M. Lawrence, P. S. Riseborough, N. O. Moreno, P. G. Pagliuso, J. L. Sarrao, J. D. Thompson, E. A. Goremychkin, F. R. Trouw, M. P. Hehlen, and R. J. McQueeney, Phys. Rev. B **70**, 134505 (2004).

[32] T. Tayama, A. Harita, T. Sakakibara, Y. Haga, H. Shishido, R. Settai, and Y. Onuki, Phys. Rev. B **65**, 180504 (2002).

[33] A. Akbari, P. Thalmeier, and I. Eremin, Phys. Rev. B **84**, 134505 (2011).

[34] A. Akbari and P. Thalmeier, Phys. Rev. Lett. **108**, 146403 (2012).

[35] A. Akbari, P. Thalmeier, and P. Fulde, Phys. Rev. Lett. **102**, 106402 (2009).